CrossMark

Well-Balanced Discontinuous Galerkin Methods for the Euler Equations Under Gravitational Fields

Gang Li[1] · **Yulong Xing**[2]

Abstract Euler equations under gravitational field admit hydrostatic equilibrium state where the flux produced by the pressure is exactly balanced by the gravitational source term. In this paper, we present well-balanced Runge–Kutta discontinuous Galerkin methods which can preserve the isothermal hydrostatic balance state exactly and maintain genuine high order accuracy for general solutions. To obtain the well-balanced property, we first reformulate the source term, and then approximate it in a way which mimics the discontinuous Galerkin approximation of the flux term. Extensive one- and two-dimensional simulations are performed to verify the properties of these schemes such as the exact preservation of the hydrostatic balance state, the ability to capture small perturbation of such state, and the genuine high order accuracy in smooth regions.

1 Introduction

Hydrodynamical evolution in a gravitational field arises in many applications from astrophysics and climate. They are usually modeled by the Euler equations governing the conservation of mass, momentum and energy, coupled with a source term due to the gravitational field. In one space dimension, they take the form of

---

✉ Yulong Xing
xingy@ucr.edu

Gang Li
gangli1978@163.com

[1] School of Mathematical Sciences, Qingdao University, Qingdao 266071, Shandong, People's Republic of China

[2] Department of Mathematics, University of California Riverside, Riverside, CA 92521, USA

$$\rho_t + (\rho u)_x = 0,$$
$$(\rho u)_t + (\rho u^2 + p)_x = -\rho \phi_x,$$
$$E_t + ((E + p)u)_x = -\rho u \phi_x, \tag{1.1}$$

where ρ denotes the fluid density, u is the velocity, p represents the pressure, and $E = \frac{1}{2}\rho u^2 + \rho e$ (e is internal energy) is the non-gravitational energy which includes the kinetic and internal energy of the fluid. γ is the ratio of specific heats and $\phi = \phi(x)$ is the time independent gravitational potential. The ideal gas law

$$p = (\gamma - 1)(E - \rho u^2/2), \tag{1.2}$$

is considered to close this system.

The Euler equations under gravitational field (1.1) belong to the class of hyperbolic equations with source terms (also referred as hyperbolic balance laws), which takes the general form of

$$U_t + F(U)_x = S(U, x), \tag{1.3}$$

where U is the solution vector with the corresponding flux $F(U)$, and $S(U, x)$ is the source term. This system usually admits non-trivial steady state solutions, in which the source term is exactly balanced by the flux gradient. One main challenge in the numerical simulation of such balance laws is that a standard numerical method may not satisfy the discrete version of this balance exactly at (or near) the steady state, and may introduce spurious oscillations, unless the mesh size is extremely refined. To save the computational cost, well-balanced methods, which preserve exactly these steady state solutions up to machine accuracy, are specially designed to ensure accurate simulations and exhibit essential stability properties on relatively coarse meshes. Another prototypical example considered extensively in the literature for hyperbolic balance laws is the shallow water equations with a non-flat bottom topology. Many researchers have developed well-balanced methods for the shallow water equations using different approaches, see, e.g. [1,2,8,10,13,18,19,23,25] and the references therein.

For the Euler equations (1.1) under static gravitation potential $\phi(x)$, there exists the hydrostatic equilibrium state, also called mechanical equilibrium, where the external forces such as gravity are balanced by the pressure gradient force:

$$\rho = \rho(x), \quad u = 0, \quad p_x = -\rho \phi_x. \tag{1.4}$$

It is difficult to design well-balanced numerical methods which can accurately preserve all the solutions of (1.4). Two important special steady state are the constant entropy (isentropic) and constant temperature (isothermal) hydrostatic equilibrium states [9]. Techniques required to balance each equilibrium can be different. In this paper, we only consider the isothermal hydrostatic balance with a constant temperature T. For an ideal gas satisfying

$$p = \rho RT, \tag{1.5}$$

where R is the gas constant, the steady state solution (1.4) becomes

$$\rho = \rho_0 \exp\left(-\frac{\phi}{RT}\right), \quad u = 0, \quad p = RT\rho = RT\rho_0 \exp\left(-\frac{\phi}{RT}\right), \tag{1.6}$$

with a constant ρ_0 after some simple calculation. The simplest and most commonly encountered case is the linear gravitational potential field with $\phi_x = g$, and the corresponding isothermal hydrostatic balance takes the form of

$$\rho = \rho_0 \exp(-g\rho_0 x/p_0), \quad u = 0, \quad p = p_0 \exp(-g\rho_0 x/p_0). \tag{1.7}$$

Many astrophysical problems involve nearly steady state flows in a gravitational field, therefore it is essential to correctly capture the effect of gravitational force in these simulations, especially if a long-time integration is involved, for example in modeling star and galaxy formation. Improper treatment of the gravitational force can lead to a solution which either oscillates around the equilibrium, or deviates from the equilibrium after a long time run. In recent years, well-balanced numerical methods for the Euler equations with gravitational fields have attracted much attention. LeVeque and Bale [11] extended the quasi-steady wave-propagation methods for the Euler equations under a static gravitational field. Finite volume well-balanced discretizations with respect to dominant hydrostatics has been proposed by Botta et al. [3] for the nearly hydrostatic flows in the numerical weather prediction. Xu and his collaborators [12,17,26] have extended the gas-kinetic scheme to the multidimensional gas dynamic equations to develop well-balanced numerical methods, where the gravitational potential was modeled as a piecewise step function with a potential jump at the cell interface. Finite volume well-balanced methods for the isentropic hydrostatic equilibrium are proposed by Kappeli and Mishra [9]. High order finite difference well-balanced methods for the isothermal equilibrium are introduced in [22] by Xing and Shu. Other related work on well-balanced methods for the Euler equations with gravitational field can be found in [4,7,27].

All of the works mentioned above are finite difference or finite volume methods. During the past few decades, high order discontinuous Galerkin (DG) method has gained great attention in solving hyperbolic conservation laws. DG method is a class of finite element methods using discontinuous piecewise polynomial space as the solution and test function spaces (see [5] for a historic review). It combines advantages of both finite element and finite volume methods, and can achieve high order of accuracy easily with the use of high order polynomials within each element. Several advantages of the DG method, including its accuracy, high parallel efficiency, flexibility for hp-adaptivity and arbitrary geometry and meshes, make it useful for a wide range of applications.

The main objective of this paper is to develop high order accurate well-balanced Runge–Kutta DG (RKDG) methods for the isothermal hydrostatic balance of Euler equations with gravitation field. This will be the first paper to achieve this goal, to our best knowledge. To achieve well-balanced property, we first rewrite the source terms in an equivalent special form using the hydrostatic balance solution (1.6). They are then discretized to be both high order accurate for general solutions and exactly well balanced with the pressure gradient at the equilibrium state. The proposed method is a generalization of well-balanced RKDG methods [20] designed for balancing the steady state solutions of the shallow water equations.

This paper is organized as follows. In Sect. 2, we first present the novel one-dimensional high order well-balanced DG method, which can preserve the isothermal hydrostatic balance solution (1.6) exactly, and at the same time is genuinely high order accurate for the general solutions. We then extend the proposed well-balanced method to multi-dimensional problems. Section 3 contains extensive numerical simulation results to demonstrate the behavior of our well-balanced DG methods for one- and two-dimensional Euler equations under gravitational field, verifying high order accuracy, the well-balanced property, and good resolution for smooth and discontinuous solutions. Some conclusions are given in Sect. 4.

2 Well-Balanced RKDG Methods

In this section, we present high order well-balanced DG methods for the steady state solution satisfying (1.6). To better illustrate the key well-balanced idea, we start by presenting numerical methods that balance a simplified version of the steady state (1.6), which takes the form of

$$\rho = c \exp(-gx), \quad u = 0, \quad p = c \exp(-gx), \tag{2.1}$$

in conjunction with the linear gravitational potential filed, i.e.,

$$\phi_x = g. \tag{2.2}$$

Extension to general steady state solution (1.6) will be discussed later in Sect. 2.3. We will confine our discussion to one dimensional problem first, again for ease of presentation, and discuss the generalization to high dimensional case at the end of this section.

2.1 Notations

We start by presenting the standard notations. We divide the interval $I = [a, b]$ into N subintervals and denote the cells by $I_j = [x_{j-\frac{1}{2}}, x_{j+\frac{1}{2}}]$ for $j = 1, \ldots, N$. The center of each cell is $x_j = \frac{1}{2}(x_{j-\frac{1}{2}} + x_{j+\frac{1}{2}})$, and the mesh size is denoted by $h_j = x_{j+\frac{1}{2}} - x_{j-\frac{1}{2}}$, with $h = \max_{1 \leq j \leq N} h_j$ being the maximal mesh size. The piecewise polynomial space V_h^k is defined as the space of polynomials of degree up to k in each cell I_j, that is,

$$V_h^k = \left\{ v : v|_{I_j} \in P^k(I_j), \ j = 1, 2, \ldots, N \right\}. \tag{2.3}$$

Note that functions in V_h^k are allowed to have discontinuities across element interfaces.

For any unknown u, its numerical approximation in the DG methods is denoted by u_h, which belongs to the finite element space V_h^k. We denote by $(u_h)_{j+\frac{1}{2}}^+$ and $(u_h)_{j+\frac{1}{2}}^-$ the limit values of u_h at $x_{j+\frac{1}{2}}$ from the right cell I_{j+1} and from the left cell I_j, respectively. The usual notations $[u_h] = u_h^+ - u_h^-$ and $\{u_h\} = \frac{1}{2}(u_h^+ + u_h^-)$ are used to represent the jump and the average of the function u_h at the element interfaces.

2.2 Well-Balanced Methods for the Simplified Steady State (2.1)

Many well-balanced methods, including DG methods, have been designed for the shallow water equations. To achieve the well-balanced property, the key idea is to introduce a numerical discretization of the source term, which mimics the approximation of the flux term, so that the exact balance between the source term and the flux can be achieved at the steady state numerically. There exist two commonly used approaches in the literature to design well-balanced DG methods for the shallow water equations. The first approach [20,23] often rewrite the equations into an equivalent way and introduce a non-standard discretization of the source term based on that. The second approach [21,23,24] employs the idea of hydrostatic reconstruction [1] to modify the approximation of numerical flux while keeping a simple source term approximation. Due to the nonlinear dependence of the isothermal steady state (2.1) on the external gravitational field $\phi(x)$, it is not easy to extend the hydrostatic reconstruction idea directly. Here, we would like to follow the first approach.

2.2.1 Reformulation of the Equation

We first reformulate the original governing equations as follows

$$\rho_t + (\rho u)_x = 0,$$
$$(\rho u)_t + \left(\rho u^2 + p\right)_x = \rho \exp(gx)(\exp(-gx))_x,$$
$$E_t + ((E + p)u)_x = -\rho u g, \tag{2.4}$$

where we replace $-\rho g$ by $\rho \exp(gx)(\exp(-gx))_x$ in the second equation, following the idea in our recent finite difference work [22]. By writing in this special form, we hope to create the derivative term in the source term, which can be treated in the similar way as the flux term at the steady state (2.1) to achieve the well-balanced property. We do not change the source term in the last equation, since the well-balanced property for this equation can be easily obtained when $u = 0$ at the steady state.

For brevity, we rewrite the Eq. (2.4) in a concise vector form

$$U_t + F(U)_x = S,$$

where $U = (\rho, \ \rho u, \ E)^T$ with the superscript T denoting the transpose, $F(U)$ represents the physical flux and S is the source term. Denote the DG approximation to the solution U by $U_h \in V_h^k$. The standard semi-discrete DG methods for (2.4) are defined as follows: for any test function $v \in V_h^k$, U_h is given by

$$\int_{I_j} (U_h)_t v \, dx - \int_{I_j} F(U_h) v_x \, dx + \hat{F}_{j+\frac{1}{2}} v \left(x_{j+\frac{1}{2}}^-\right) - \hat{F}_{j-\frac{1}{2}} v \left(x_{j-\frac{1}{2}}^+\right) = \int_{I_j} S v \, dx, \tag{2.5}$$

where

$$\widehat{F}_{j+\frac{1}{2}} = f \left(U_h \left(x_{j+\frac{1}{2}}^-, t\right), U_h \left(x_{j+\frac{1}{2}}^+, t\right)\right), \tag{2.6}$$

and $f(a_1, a_2)$ is a numerical flux. One example is the simple Lax-Friedrichs flux

$$f(a_1, a_2) = \frac{1}{2}(F(a_1) + F(a_2) - \alpha(a_2 - a_1)), \tag{2.7}$$

where $\alpha = \max \lambda(u)$ with $\lambda(u)$ being the eigenvalues of the Jacobian $F'(U)$, and the maximum is taken over the whole region.

2.2.2 Novel Source Term Approximation

The standard DG methods (2.5) alone do not have the well-balanced property. To preserve the steady state solution (2.1), we need to introduce a non-standard approximation to the source term integral. The function $\exp(-gx)$ appears in the source term S, and we introduce the notation

$$b(x) = \exp(-gx),$$

for ease of presentation. We first decompose the integral of the source term in the second equation as

$$\int_{I_j} S_2 v dx = \int_{I_j} \rho \exp(gx) \left(\exp(-gx)\right)_x v dx = \int_{I_j} \frac{\rho}{b} b_x v dx \tag{2.8}$$

$$= \frac{\rho(x_j)}{b(x_j)} \left(b\left(x_{j+\frac{1}{2}}^-\right) v\left(x_{j+\frac{1}{2}}^-\right) - b\left(x_{j-\frac{1}{2}}^+\right) v\left(x_{j-\frac{1}{2}}^+\right) - \int_{I_j} b v_x dx \right)$$

$$+ \int_{I_j} \left(\frac{\rho}{b} - \frac{\rho(x_j)}{b(x_j)} \right) b_x v dx.$$

In Remark 1 below, we provide some explanations on why such decomposition is needed for the purpose of well-balancedness, and introduce some other alternative equivalent decompositions.

We now project $b(x)$ into the piecewise polynomial space V_h^k, to obtain the polynomial $b_h(x)$, using the standard L^2 projection. Our numerical approximation to the source term (2.8) takes the form of

$$\int_{I_j} S_2 v dx \approx \int_{I_j} \left(\frac{\rho_h}{b_h} - \frac{\rho_h(x_j)}{b_h(x_j)} \right) (b_h)_x v dx$$

$$+ \frac{\rho_h(x_j)}{b_h(x_j)} \left(\{b_h\} \left(x_{j+\frac{1}{2}}\right) v\left(x_{j+\frac{1}{2}}^-\right) - \{b_h\} \left(x_{j-\frac{1}{2}}\right) v\left(x_{j-\frac{1}{2}}^+\right) - \int_{I_j} b_h v_x dx \right), \tag{2.9}$$

where ρ, b are replaced by the DG approximations ρ_h, b_h, and the boundary values of b_h are replaced by the average of b_h at the cell interface, denoted by $\{b_h\}$, to be consistent with the numerical flux $\hat{F}_{j\pm1/2}$. For the integral of the source term in the third equation, we simply approximate it by

$$\int_{I_j} S_3 v dx \approx \int_{I_j} -(\rho u)_h g v dx, \tag{2.10}$$

where the standard quadrature rule is used to evaluate this integral.

2.2.3 Well-Balanced Numerical Fluxes

The last piece in designing well-balanced DG methods is to modify the numerical flux $\hat{F}_{j+1/2}$. The term $\alpha(a_2 - a_1)$ in the Lax-Friedrichs flux (2.7) contributes to the numerical viscosity term, which is essential for this nonlinear conservation laws. However they will destroy the well-balanced property at the steady state. We propose to modify it as

$$\hat{F}_{j+1/2} = \frac{1}{2} \left[F\left(U_h\left(x_{j+1/2}^-, t\right)\right) + F\left(U_h\left(x_{j+1/2}^+, t\right)\right) \right.$$

$$\left. -\alpha' \left(\frac{U_h\left(x_{j+1/2}^+, t\right)}{b_h\left(x_{j+1/2}^+\right)} - \frac{U_h\left(x_{j+1/2}^-, t\right)}{b_h\left(x_{j+1/2}^-\right)} \right) \right], \tag{2.11}$$

where the coefficient α' is defined as

$$\alpha' = \alpha \max_x b_h(x), \tag{2.12}$$

to maintain enough artificial numerical viscosity. This modification does not affect the accuracy, but at the steady state (2.1), the term U_h/b_h becomes a constant. Therefore, the effect

of these viscosity terms becomes zero and the numerical flux now reduces to a simple form

$$\widehat{F}_{j+\frac{1}{2}} = \frac{1}{2}\left[F\left(U\left(x_{j+\frac{1}{2}}^-, t\right)\right) + F\left(U\left(x_{j+\frac{1}{2}}^+, t\right)\right)\right].\tag{2.13}$$

2.2.4 Well-Balanced Methods

All these together lead to a well-balanced DG method for the Euler equations, as outlined in the following proposition.

Proposition 1 *For the Euler equations* (1.1) *with the linear gravitational potential field* (2.2)*, the semi-discrete DG methods* (2.5)*, combined with* (2.9)*,* (2.10) *and* (2.11)*, are well-balanced for the steady state solution* (2.1)*.*

Proof At the steady state (2.1), we have

$$\rho_h = cb_h, \qquad u = 0, \qquad p_h = cb_h.$$

Easy to observe that the well-balanced property holds for the first and third equations, as both the flux and source term approximations in these equations become zero. For the momentum equation, we have $\rho_h(x_j)/b_h(x_j) = \rho_h(x)/b_h(x) \equiv c$, and the source term approximation (2.9) becomes

$$\int_{I_j} S_2 v \, dx \approx c\left(\{b_h\}\left(x_{j+\frac{1}{2}}\right)v\left(x_{j+\frac{1}{2}}^-\right) - \{b_h\}\left(x_{j-\frac{1}{2}}\right)v\left(x_{j-\frac{1}{2}}^+\right) - \int_{I_j} b_h v_x \, dx\right).\tag{2.14}$$

Since $u = 0$, the flux term $F_2 = \rho u^2 + p$ reduces to p. Utilizing (2.13) and the equilibrium $p_h = cb_h$, its numerical approximation takes the form of

$$\hat{F}_2\left(x_{j+\frac{1}{2}}\right)v\left(x_{j+\frac{1}{2}}^-\right) - \hat{F}_2\left(x_{j-\frac{1}{2}}\right)v\left(x_{j-\frac{1}{2}}^+\right) - \int_{I_j} F_2 v_x \, dx$$

$$= c\{b_h\}\left(x_{j+\frac{1}{2}}\right)v\left(x_{j+\frac{1}{2}}^-\right) - c\{b_h\}\left(x_{j-\frac{1}{2}}\right)v\left(x_{j-\frac{1}{2}}^+\right) - \int_{I_j} cb_h v_x \, dx.\tag{2.15}$$

We can conclude that the flux and source term approximations balance each other, which leads to the well-balanced property of our methods. □

Remark 1 The choice of $\rho_h(x_j)/b_h(x_j)$ in (2.9) is not unique, and can be replace by any other term that can recover constant c at the steady state (1.6), for example, $\overline{(\rho_h)}_j/\overline{(b_h)}_j$. We would like to comment that although $\rho \exp(gx) = c$ at the steady state (2.1), this equality does not hold for the product of two polynomials which approximate these functions, i.e., $\rho_h \exp(gx)_h \neq c$ everywhere pointwise (where $\exp(gx)_h$ stands for the L^2 projection of $\exp(gx)$ into the space V_h^k).

Remark 2 A straightforward way to approximate the source term (2.8) by:

$$\int_{I_i} \rho \exp(gx) \left(\exp(-gx)\right)_x v \, dx$$

$$= \rho\left(x_{i+1/2}^-\right)v\left(x_{i+1/2}^-\right) - \rho\left(x_{i-1/2}^+\right)v\left(x_{i-1/2}^+\right) - \int_{I_i} \exp(-gx)\left(\frac{\rho}{\exp(-gx)}v\right)_x \, dx,\tag{2.16}$$

and then change ρ, $\exp(-gx)$ to ρ_h, b_h, and replace the cell boundary value of ρ_h by $\{\rho_h\}$, seems to work by repeating the proof of Proposition 1. One main concern in taking this source term approximation is that the derivative of the unknown ρ appears in the source term approximation, and the flux $\{\rho_h\}$ is introduced at the cell interface to communicate with neighboring cells, which may violate the Lax-Wendroff theorem, hence affect the convergence towards the weak solution when discontinuous solutions appear. For example, when no source term presents, i.e., $g = 0$, the source term approximation (2.9) vanishes, while the approximation (2.16) does not (if one replaces the cell boundary value of ρ_h by $\{\rho_h\}$ in (2.16)).

2.2.5 Temporal Discretization and Slope Limiter

For the temporal discretization, high order total variation diminishing (TVD) Runge–Kutta methods [15] can be used. In the numerical section of this paper, we apply the third order Runge–Kutta methods:

$$
\begin{aligned}
U_h^{(1)} &= U_h^n + \Delta t \mathcal{F}\left(U_h^n\right) \\
U_h^{(2)} &= \frac{3}{4} U_h^n + \frac{1}{4}\left(U_h^{(1)} + \Delta t \mathcal{F}\left(U_h^{(1)}\right)\right) \\
U_h^{n+1} &= \frac{1}{3} U_h^n + \frac{2}{3}\left(U_h^{(2)} + \Delta t \mathcal{F}\left(U_h^{(2)}\right)\right),
\end{aligned}
\tag{2.17}
$$

with $\mathcal{F}(U_h)$ being the spatial operator.

When the solution contains discontinuities, slope limiter procedure is usually needed for the DG methods. They are applied after each inner stage of the Runge–Kutta methods. Many different choices of slope limiters have been presented in the literature. In this paper, we consider the total variation bounded (TVB) limiter presented in [6,14]. This limiter procedure itself might destroy the well-balanced property, and violate the exact preservation of the steady state (2.1).

Here we follow the idea presented in [24] and propose the following well-balanced way to perform the TVB limiter. Usually, when we perform the TVB limiter on the unknowns U_h, it involves two steps. The first step is to check whether any limiting is needed in the cell I_j based on the cell averages $(\bar{U}_h)_j$, $(\bar{U}_h)_{j\pm1}$ and $(U_h)_{j+1/2}^-$, $(U_h)_{j-1/2}^+$. If the answer is positive, the second step is to apply the TVB limiter on the variables U_h in this cell I_j. To present well-balanced slope limiter procedure, we propose to first check if the limiting is needed based on the cell averages $(\overline{U_h/b_h})_j$, $(\overline{U_h/b_h})_{j\pm1}$ and $(U_h/b_h)_{j+1/2}^-$, $(U_h/b_h)_{j-1/2}^+$. If one cell is determined as needing limiting, we apply the actual TVB limiter on U_h as usual. Note that U_h/b_h becomes constant at the steady state (2.1). When the limiting procedure is implemented this way, if the steady state is reached, no cell will be flagged as requiring limiting, hence we do not apply any TVB limiter and therefore the well-balanced property is maintained.

2.3 Well-Balanced Methods for the General Steady State (1.6)

Well-balanced DG methods have been designed for the special steady state (2.1) in the previous subsection. In the subsection, we extend these methods to the more general steady state (1.6) with the gravitational field $\phi(x)$. We first rewrite the governing Eq. (1.1) as

$$\rho_t + (\rho u)_x = 0,$$
$$(\rho u)_t + \left(\rho u^2 + p\right)_x = RT\rho \exp\left(\frac{\phi}{RT}\right)\left(\exp\left(-\frac{\phi}{RT}\right)\right)_x,$$
$$E_t + ((E+p)u)_x = -\rho u g, \tag{2.18}$$

which is the analogy of the Eq. (2.4) for the special steady state (2.1).

The semi-discrete well-balanced DG methods still take the form of (2.5), but with a modified flux and source term approximations outlined below. For ease of presentation, we introduce the notation

$$d(x) = \exp\left(-\frac{\phi}{RT}\right),$$

and denote its projection in the space V_h^k as $d_h(x)$. Following the same technique as stated above, we decompose the integral of the source term in the second equation as

$$\int_{I_j} S_2 v \mathrm{d}x = \int_{I_j} RT\rho \exp\left(\frac{\phi}{RT}\right)\left(\exp\left(-\frac{\phi}{RT}\right)\right)_x v\mathrm{d}x = \int_{I_j} \frac{RT\rho}{d} d_x v\mathrm{d}x$$
$$= RT\frac{\rho(x_j)}{d(x_j)}\left(d\left(x_{j+\frac{1}{2}}^-\right)v\left(x_{j+\frac{1}{2}}^-\right) - d\left(x_{j-\frac{1}{2}}^+\right)v\left(x_{j-\frac{1}{2}}^+\right) - \int_{I_j} dv_x\mathrm{d}x\right)$$
$$+ \int_{I_j} RT\left(\frac{\rho}{d} - \frac{\rho(x_j)}{d(x_j)}\right)d_x v\mathrm{d}x, \tag{2.19}$$

and approximate it by

$$\int_{I_j} S_2 v\mathrm{d}x \approx \int_{I_j} RT\left(\frac{\rho_h}{d_h} - \frac{\rho_h(x_j)}{d_h(x_j)}\right)(d_h)_x v\mathrm{d}x$$
$$+ RT\frac{\rho_h(x_j)}{d_h(x_j)}\left(\{d_h\}\left(x_{j+\frac{1}{2}}\right)v\left(x_{j+\frac{1}{2}}^-\right) - \{d_h\}\left(x_{j-\frac{1}{2}}\right)v\left(x_{j-\frac{1}{2}}^+\right) - \int_{I_j} d_h v_x\mathrm{d}x\right), \tag{2.20}$$

where ρ, d are replaced by the DG approximations ρ_h, d_h, and the boundary values of d_h are replaced by the cell average $\{d_h\}$. The integral of the source term in the third equation is still approximated by (2.10), and the numerical flux takes the same form as in (2.11), with b_h replaced by d_h.

Following the same proof, we can show that the semi-discrete DG methods (2.5), combined with (2.20), (2.10) and (2.11) (with b_h replaced by d_h), are well-balanced for the general steady state solution (1.6) with the gravitational field $\phi(x)$.

2.4 Extension to Multi-dimensional Case

In this subsection, we extend well-balanced DG methods to multi-dimensional Euler equations with the gravitational field ϕ. The governing equations have the following formulation

$$\rho_t + \nabla \cdot (\rho\mathbf{u}) = 0,$$
$$(\rho\mathbf{u})_t + \nabla \cdot (\rho\mathbf{u} \otimes \mathbf{u} + p\mathbf{I}_d) = -\rho\nabla\phi,$$
$$E_t + \nabla \cdot ((E+p)\mathbf{u}) = -\rho\mathbf{u} \cdot \nabla\phi, \tag{2.21}$$

where $\mathbf{x} \in \mathcal{R}^l$ ($l = 2, 3$) is the spatial variable, ρ, $\mathbf{u}$, p denote the density, velocity, and pressure. $E = \frac{1}{2}\rho\|\mathbf{u}\|^2 + p/(\gamma - 1)$ is the non-gravitational energy. The operators ∇, $\nabla\cdot$ and $\otimes$ are the gradient, divergence and tensor product in $\mathcal{R}^l$, respectively.

Here we are interested in maintaining the steady state solution with the constant temperature T and the zero velocity, given by

$$\rho = \rho_0 \exp\left(-\frac{\phi}{RT}\right), \quad \mathbf{u} = 0, \quad p = RT\rho = RT\rho_0 \exp\left(-\frac{\phi}{RT}\right). \qquad (2.22)$$

In the special case of linear gravitational potential field $\phi(\mathbf{x}) = \mathbf{g} \cdot \mathbf{x}$, the corresponding steady state solutions takes the form of

$$\rho = \rho_0 \exp\left(-\rho_0(\mathbf{g} \cdot \mathbf{x})/p_0\right), \quad u = v = 0, \quad p = p_0 \exp\left(-\rho_0(\mathbf{g} \cdot \mathbf{x})/p_0\right).$$

Let $\mathcal{T}_\tau$ be a family of partitions of the computational domain Ω parameterized by $\tau > 0$. We do not specify the mesh element here. In two dimension, well-balanced DG methods proposed below work for both rectangular and triangular meshes. For any element $K \in \mathcal{T}_\tau$, we define $\tau_K := \mathrm{diam}(K)$ and $\tau := \max_{K \in \mathcal{T}_\tau} \tau_K$. For each edge e_K^i ($i = 1, \ldots, m$) of K, we denote the outward unit normal vector by ν_K^i and the area of the element K by $|K|$.

Let us denote the multi-dimensional Euler equations (2.21) by

$$\mathbf{U}_t + \nabla \cdot \mathbf{F}(U) = S,$$

where $\mathbf{U} = (\rho, \rho\mathbf{u}, E)^T$, $\mathbf{F}(\mathbf{U})$ is the flux and S is the source term. The DG approximation $\mathbf{U}_h$ belongs to the finite dimensional space

$$V_\tau^k \equiv \{w \in L^2(\Omega); \ w|_K \in P^k(K) \ \forall K \in \mathcal{T}_\tau\}, \qquad (2.23)$$

where $P^k(K)$ denotes the space of polynomials on the element K with at most k-th degree. The semi-discrete DG method is given by

$$\int_K \partial_t \mathbf{U} w \, \mathrm{d}\mathbf{x} - \int_K \mathbf{F}(\mathbf{U}) \cdot \nabla w \, \mathrm{d}\mathbf{x} + \sum_{i=1}^m \int_{e_K^i} \widehat{\mathbf{F}}|_{e_K^i} \cdot \nu_K^i w \, \mathrm{d}s = \int_K S w \, \mathrm{d}\mathbf{x}, \qquad (2.24)$$

where $w(\mathbf{x})$ is a test function from the test space V_τ^k. The numerical flux $\widehat{\mathbf{F}}$ is defined by

$$\widehat{\mathbf{F}}|_{e_K^i} \cdot \nu_K^i = \mathcal{F}\left(U_i^{int(K)}, U_i^{ext(K)}, \nu_K^i\right). \qquad (2.25)$$

where $U_i^{int(K)}$ and $U_i^{ext(K)}$ are the approximations to the values on the edge e_K^i obtained from the interior and the exterior of K. The simple global Lax-Friedrichs flux takes the form of

$$\mathcal{F}(a_1, a_2, \nu) = \frac{1}{2}\left[\mathbf{F}(a_1) \cdot \nu + \mathbf{F}(a_2) \cdot \nu - \alpha(a_2 - a_1)\right]. \qquad (2.26)$$

We can extend the well-balanced DG methods designed in Sect. 2.3 to multiple space dimensions. Following the steps in one-dimensional case, we first introduce the notation

$$d(\mathbf{x}) = \exp\left(-\frac{\phi(\mathbf{x})}{RT}\right), \qquad (2.27)$$

and rewrite the source term in the momentum equation of (2.21) as

$$-\rho\nabla\phi = RT\rho \exp\left(\frac{\phi}{RT}\right)\nabla\left(\exp\left(-\frac{\phi}{RT}\right)\right) = \frac{RT\rho}{d}\nabla d. \qquad (2.28)$$

The well-balanced approximation to the integral of this source term follows an analogue of the decomposition (2.19), which leads to

$$\int_K S_2 w \, \mathrm{d}\mathbf{x} = \int_K \frac{RT\rho}{d} \nabla d \, w \, \mathrm{d}\mathbf{x} \tag{2.29}$$

$$= RT \frac{\rho\left(\mathbf{x}_K^0\right)}{d\left(\mathbf{x}_K^0\right)} \left(\sum_{i=1}^{m} \int_{e_K^i} d\left(\mathbf{x}_i^{int(K)}\right) v_K^i w \, \mathrm{d}s - \int_K d \, \nabla w \, \mathrm{d}\mathbf{x} \right)$$

$$+ \int_K RT \left(\frac{\rho}{d} - \frac{\rho\left(\mathbf{x}_K^0\right)}{d\left(\mathbf{x}_K^0\right)} \right) \nabla d \, w \, \mathrm{d}\mathbf{x},$$

where $\mathbf{x}_K^0$ stands for the middle point or arbitrary point within the element K that is easy to evaluate. We approximate the source term (2.29) by

$$\int_K S_2 w \, \mathrm{d}\mathbf{x} \approx \int_K RT \left(\frac{\rho_h}{d_h} - \frac{\rho_h\left(\mathbf{x}_K^0\right)}{d_h\left(\mathbf{x}_K^0\right)} \right) \nabla d_h \, w \, \mathrm{d}\mathbf{x}$$

$$+ RT \frac{\rho_h\left(\mathbf{x}_K^0\right)}{d_h\left(\mathbf{x}_K^0\right)} \left(\sum_{i=1}^{m} \int_{e_K^i} \{d_h(\mathbf{x})\} v_K^i w \, \mathrm{d}s - \int_K d_h \, \nabla w \, \mathrm{d}\mathbf{x} \right), \tag{2.30}$$

where ρ, d are replaced by the DG approximations ρ_h, d_h, and the boundary values of d_h are replaced by the cell average $\{d_h\}$. The last piece in designing the well-balanced DG methods is to replace the Lax-Friedrichs numerical flux (2.25)–(2.26) by:

$$\widehat{\mathbf{F}}|_{e_K^i} \cdot v_K^i = \frac{1}{2} \left[\mathbf{F}\left(U_i^{int(K)}\right) \cdot v_K^i + \mathbf{F}\left(U_i^{ext(K)}\right) \cdot v_K^i \right.$$

$$\left. -\alpha' \left(\frac{U_i^{ext(K)}}{d_h\left(\mathbf{x}_i^{ext(K)}\right)} - \frac{U_i^{int(K)}}{d_h\left(\mathbf{x}_i^{int(K)}\right)} \right) \right]. \tag{2.31}$$

where the coefficient α' is defined as

$$\alpha' = \alpha \max_{\mathbf{x}} d_h(\mathbf{x}), \tag{2.32}$$

to maintain enough artificial numerical viscosity. All these together lead to a well-balanced DG method for the Euler equations, as outlined in the following proposition.

Proposition 2 *For the multi-dimensional Euler equations* (2.21) *with the gravitational potential field* $\phi(\mathbf{x})$, *the semi-discrete DG methods* (2.24), *combined with* (2.30) *and* (2.31), *are well-balanced for the steady state solution* (2.22).

3 Numerical Results

In this section, we carry out extensive one- and two-dimensional numerical experiments to demonstrate the performance of the proposed well-balanced RKDG methods. In all the computations, we use the third order TVD Runge–Kutta methods (2.17), coupled with third order finite element DG methods (i.e., $k = 2$). The CFL number is taken as 0.18.
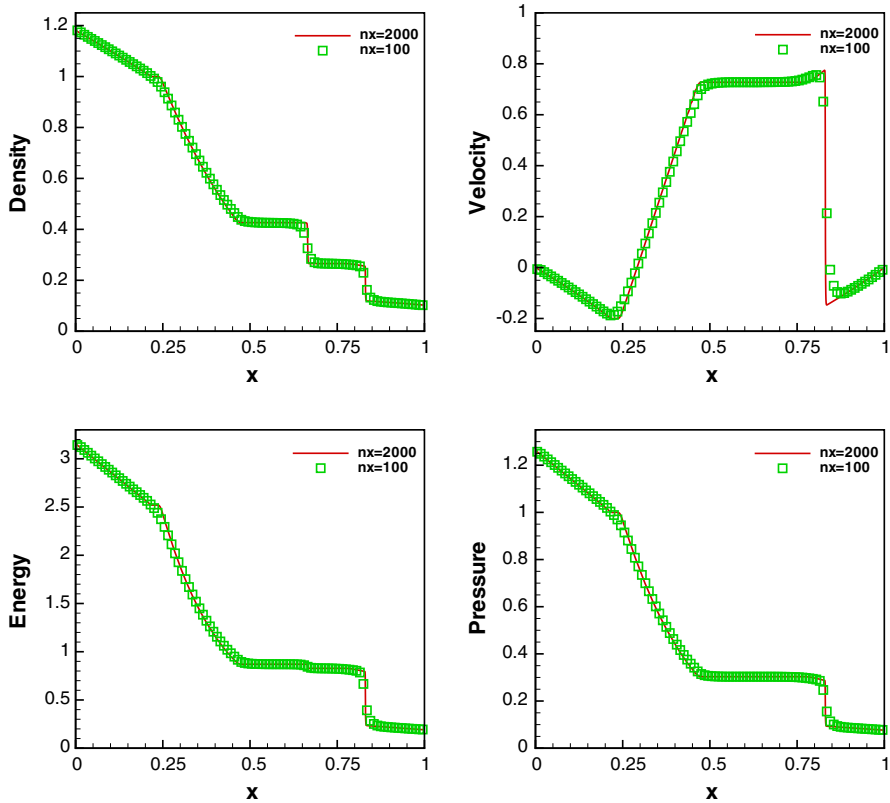
Fig. 1 The numerical solutions of the shock tube problem under gravitational field in Sect. 3.1 at time $t = 0.2$. *Top left* density distribution, *top right* velocity distribution, *bottom left* energy distribution, *bottom right* pressure distribution

3.1 One-Dimensional Shock Tube Problem Under Gravitational Field

In this standard Sod test, the discontinuous initial conditions are given by

$$(\rho, v, p) = \begin{cases} (1, 0, 1) & \text{if } x \leq 0.5, \\ (0.125, 0, 0.1) & \text{otherwise,} \end{cases}$$

on a unit computational domain $[0, 1]$, with a constant gravitational field $g = \phi_x = 1$ acting in the negative x direction. We compute this problem up to $t = 0.2$.

We present the numerical results compared with the reference solutions obtained with a much refined 2000 uniform cells in Fig. 1. Due to the presence of the gravitational force, the density distribution is pulling towards the left direction, and negative velocity appears in some regions. By comparing the results in these figures, we can clearly observe that the numerical results capture sharp discontinuity transition even on a relatively coarse mesh with 100 cells, and agree well with the reference solutions.

Table 1 L^1 errors for different precisions for the steady state solution (3.1) in Sect. 3.2

N	Precision	ρ	ρu	E
100	Single	2.38E-7	2.23E-7	4.55E-7
	Double	1.76E-15	1.77E-15	1.24E-15
200	Single	3.13E-7	2.34E-7	4.31E-7
	Double	2.99E-15	1.61E-15	1.84E-15

3.2 One-Dimensional Isothermal Equilibrium Solution

In this test case, used in [11,17,22], we test the well-balanced property of the proposed DG methods for an ideal gas with $\gamma = 1.4$ under the linear gravitational field $\phi_x = g = 1$. The isothermal steady state solution is given by

$$\rho_0(x) = p_0(x) = \exp(-x) \quad \text{and} \quad u_0(x) = 0, \tag{3.1}$$

which is in the form of the special steady state (2.1). The computational domain is set as [0, 1].

We first show an example to demonstrate the well-balanced property of the proposed DG methods. The initial condition is taken as the steady state solution (3.1) which should be exactly preserved by any well-balanced method. In order to demonstrate that the steady state is indeed maintained up to the round-off error, we use single precision and double precision respectively to perform the computation. We compute the solution until $t = 2$ using both 100 and 200 uniform mesh cells, and present the L^1 errors of numerical solutions in Table 1. It can be clearly observed that the numerical errors are all at the level of round-off error for different precisions, which verifies the desired well-balanced property accordingly.

Next, we demonstrate the advantage of well-balanced methods by simulating a small perturbation of the isothermal steady state solution (3.1). We keep the density and velocity, but modify the initial pressure state to

$$p(x, t = 0) = p_0(x) + \eta \exp(-100(x - 0.5)^2),$$

where η is a non-zero perturbation parameter. Two cases, $\eta = 0.01$ and $\eta = 0.0001$, have been considered. In Fig. 2, we present the pressure perturbations at $t = 0.25$ on a mesh with 200 cells, and a reference solution obtained with a much refined 2000 cells. The initial pressure perturbation is also included as a dashed line. In addition, we run the same numerical test using the non-well-balanced DG methods, with a straightforward integration of the source term, and show their results in Fig. 2 for comparison. It is obvious that the results of well-balanced DG methods are in good agreement with the reference solutions for both cases, while non-well-balanced DG methods only provide good results for the big perturbation, but fail to capture the small perturbation with 200 cells. This demonstrates the importance of well-balanced methods in capturing small perturbations to equilibrium states.

3.3 One-Dimensional Gas Falling into a Fixed External Potential

Next, we consider a more general gravitational field, which takes the sine wave form:

$$\phi(x) = -\phi_0 \frac{L}{2\pi} \sin \frac{2\pi x}{L},$$
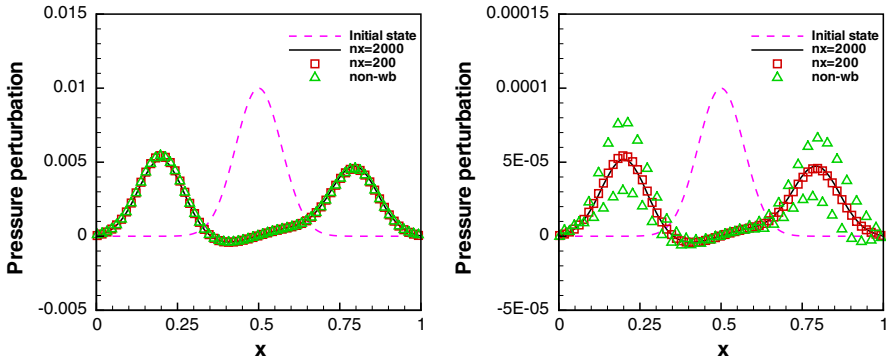
Fig. 2 The pressure perturbation of a hydrostatic solution in Sect. 3.2. The result of the well-balanced method with 200 and 2000 cells, and that of the non-well-balanced (denoted by non-wb) method with 200 cells. *Left* $\eta = 0.01$, *right* $\eta = 0.0001$

Table 2 L^1 errors for different precisions for the steady state solution (3.2) in Sect. 3.3

N	Precision	ρ	ρu	E
100	Single	1.98E-7	2.86E-7	3.03E-7
	Double	1.90E-15	5.37E-16	8.80E-16
200	Single	1.24E-7	2.65E-7	2.51E-7
	Double	2.49E-15	7.78E-16	1.20E-15

where L is the computational domain length and ϕ_0 is the amplitude. This test case was first considered in [16] and later used in [17,22]. The general steady state takes the following form

$$\rho = \rho_0 \exp\left(-\frac{\phi}{RT}\right), \quad u = 0 \quad \text{and} \quad p = RT\rho_0 \exp\left(-\frac{\phi}{RT}\right), \tag{3.2}$$

with a constant temperature T.

We first verify the well-balanced property of the the proposed DG methods. For an ideal gas with $\gamma = 5/3$, the initial conditions are defined in (3.2) with parameters $\rho_0 = 1$, $R = 1$, $T = 0.6866$, $L = 64$ and $\phi_0 = 0.02$. We compute the example up to $t = 50$ using both 100 and 200 uniform cells. We apply both single and double precisions, to carry out the computation. L^1 errors of ρ, ρu and E are presented in Table 2, where we can clearly observe that the errors are all at the level of round-off error for different precisions.

In the following test case, we impose a small perturbation to the steady state (1.6), and let the solution run for a long time. Eventually, it will converge to an isothermal hydrostatic state. We would like to compare the performance of well-balanced and non-well-balanced methods for this test.

We define the initial data as

$$\rho = \rho_0 \exp\left(-\frac{\phi}{RT}\right), \quad u = 0, \quad p = RT\rho_0 \exp\left(-\frac{\phi}{RT}\right) + 0.001 \exp\left(-10(x - 32)^2\right),$$

with the same parameters used in the well-balanced test. We run the simulation for 1, 000, 000 time steps with 64 uniform cells, and show the numerical results at the final time in Fig. 3. For comparison, we also plot the numerical results by the non-well-balanced DG methods. Easy to observe that the constant velocity and constant temperature distributions of the
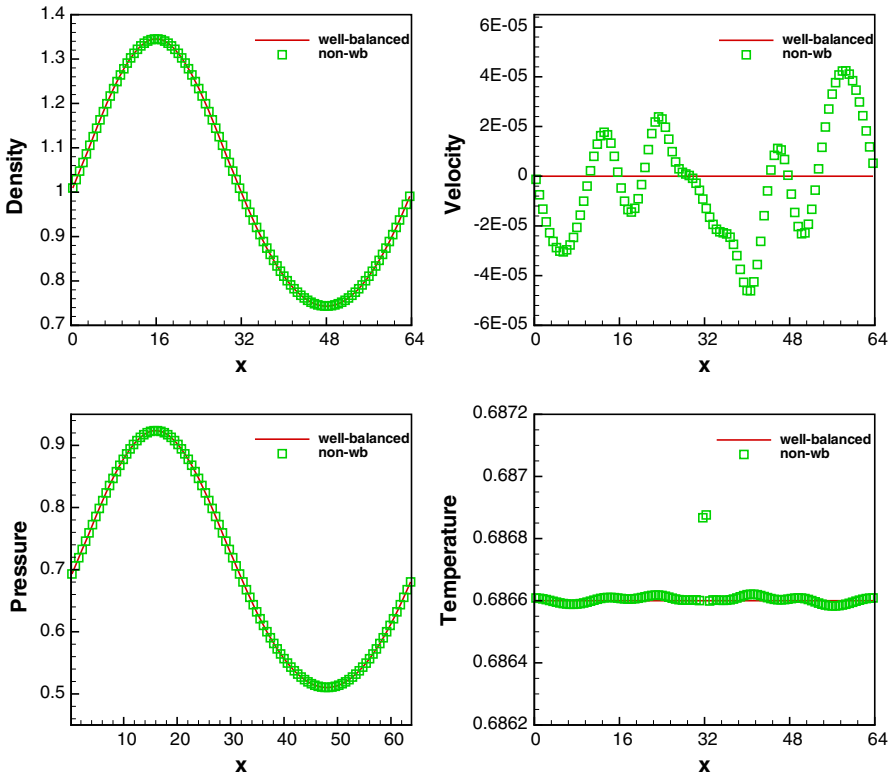
Fig. 3 The numerical solutions of well-balanced method (*solid line*) and non-well-balanced method (*square box*, denoted by non-wb) for the convergence test in Sect. 3.3 after 1,000,000 time steps. *Top left* density distribution, *top right* velocity distribution, *bottom left* pressure distribution, *bottom right* temperature distribution

equilibrium state are well-captured by the proposed well-balanced DG methods, while the non-well-balanced methods fail to achieve this.

3.4 Two-Dimensional Accuracy Test

In this two-dimensional example, we test the convergence rate of well-balanced DG methods for the Euler equations (2.21) with a linear gravitational field $\phi_x = \phi_y = 1$. For such linear field, a time-dependent exact solution has been proposed in [22], which takes the form of

$$\rho(x, y, t) = 1 + 0.2 \sin(\pi(x + y - t(u_0 + v_0))),$$
$$u(x, y, t) = u_0, \quad v(x, y, t) = v_0,$$
$$p(x, y, t) = p_0 + t(u_0 + v_0) - x - y + 0.2 \cos(\pi(x + y - t(u_0 + v_0)))/\pi,$$

on a square domain $[0, 2] \times [0, 2]$. The constants are set as $u_0 = v_0 = 1$ and $p_0 = 4.5$ in this test case. The exact solutions are taken as the boundary condition when needed. We run the simulation up to $t = 0.1$. The L^1 errors and orders of accuracy are shown in Table 3. We can clearly observe that the expected high order accuracy is achieved for the proposed well-balanced DG methods.

Table 3 L^1 errors and numerical orders of accuracy for the example in Sect. 3.4

Cells	ρ		ρu		ρv		E	
	L^1 error	Order	L^1 error	Order	L^1 error	Order	L^1 error	Order
8×8	1.20E-04		1.09E-04		1.09E-04		2.84E-04	
16×16	1.19E-05	3.33	1.13E-05	3.27	1.13E-05	3.27	3.18E-05	3.16
32×32	1.14E-06	3.39	1.17E-06	3.27	1.17E-06	3.27	3.61E-06	3.14
64×64	1.35E-07	3.07	1.58E-07	2.89	1.58E-07	2.89	4.10E-07	3.14
128×128	1.80E-08	2.91	2.15E-08	2.88	2.15E-08	2.88	4.78E-08	3.10
256×256	2.41E-09	2.90	2.94E-09	2.87	2.94E-09	2.87	5.93E-09	3.01

Table 4 L^1 errors for different precisions for the steady state solution (3.3) in Sect. 3.5

Precision	ρ	ρu	ρv	E
Single	1.35E-8	2.13E-8	2.07E-8	2.15E-8
Double	8.37E-14	6.24E-14	8.51E-14	3.27E-14

3.5 Two-Dimensional Isothermal Equilibrium Solution

We use this test case, taken from [22], to demonstrate the well-balanced property and the capacity of the proposed methods for capturing the small perturbation of an isothermal equilibrium solution in the two-dimensional case. Consider an ideal gas with $\gamma = 1.4$ and the linear gravitational field $\phi_x = \phi_y = g$. On a unit square domain, we are interested in the following isothermal equilibrium state

$$\rho(x) = \rho_0 \exp\left(-\frac{\rho_0 g}{p_0}(x + y)\right),$$
$$u(x, y) = v(x, y) = 0,$$
$$p(x, y) = p_0 \exp\left(-\frac{\rho_0 g}{p_0}(x + y)\right), \tag{3.3}$$

with $\rho_0 = 1.21$, $p_0 = 1$ and $g = 1$.

We first test the well-balanced property by using this equilibrium state as the initial data. We compute the solution up to $t = 1$ on a mesh with 50×50 uniform cells. In order to demonstrate that the steady state is indeed maintained up to round-off error, we use single precision and double precision to carry out the computation. The L^1 errors of ρ, ρu, ρv and E are shown in Table 4, where the well-balanced property can be easily observed.

Next, we demonstrate the advantage of well-balanced methods by imposing a small perturbation to the pressure state of the isothermal equilibrium solution:

$$p(x, y, t = 0) = p_0 \exp\left(-\frac{\rho_0 g}{p_0}(x + y)\right) + \eta \exp\left(-\frac{\rho_0 g}{p_0}\left((x - 0.3)^2 + (y - 0.3)^2\right)\right),$$

where $\eta = 0.001$ is a non-zero perturbation constant. We compute the example with both well-balanced DG methods and non-well-balanced methods (with a straightforward calculation of the source term), up to $t = 0.15$ with 50×50 cells and simple transmissive boundary conditions. The contour plots of their pressure perturbation are shown in Fig. 4 and the 3D figures of the pressure perturbation are shown in Fig. 5. We also include the density perturbations in Fig. 6. From these figures, we can observe that non-well-balanced DG
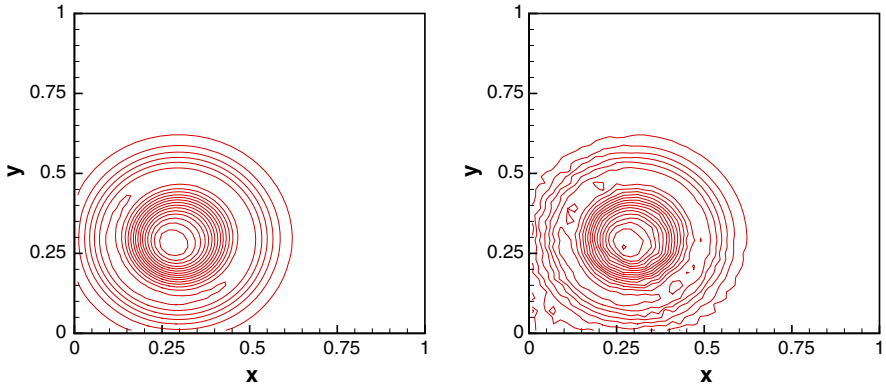
Fig. 4 The contours of the pressure perturbation of a two-dimensional hydrostatic solution in Sect. 3.5 at time $t = 0.15$ with 50×50 cells. 20 uniformly spaced contour lines from 0.0003 to 0.0003. *Left* results based on well-balanced method, *right* results based on non-well-balanced method
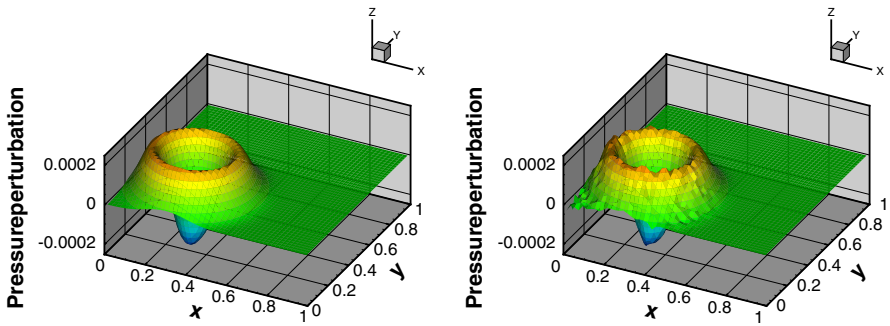
Fig. 5 The 3D figure of the pressure perturbation of a two-dimensional hydrostatic solution in Sect. 3.5 at time $t = 0.15$ with 50×50 cells. *Left* results based on well-balanced method, *right* results based on non-well-balanced method
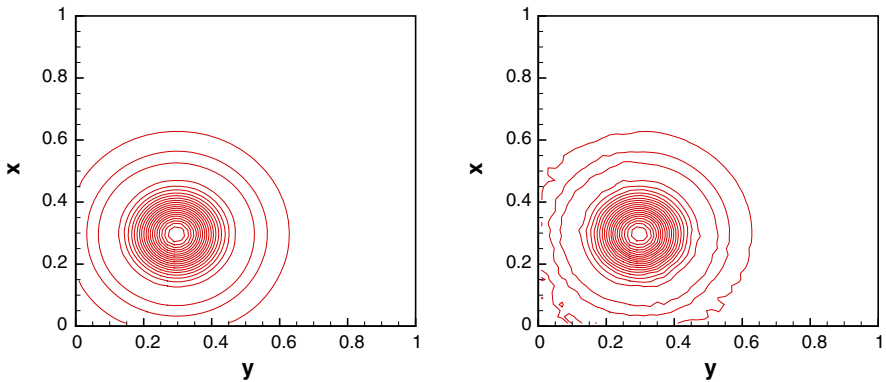
Fig. 6 The contours of the density perturbation of a two-dimensional hydrostatic solution in Sect. 3.5 at time $t = 0.15$ with 50×50 cells. 20 uniformly spaced contour lines from -0.001 to 0.0002. *Left* results based on well-balanced method, *right* results based on non-well-balanced method
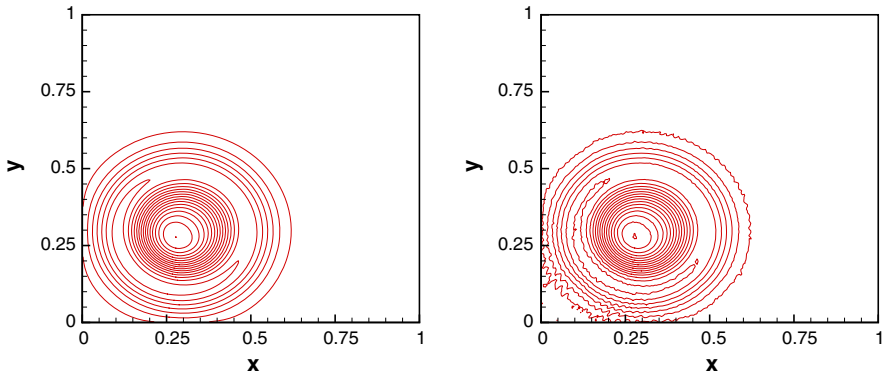
Fig. 7 The contours of the pressure perturbation of a two-dimensional hydrostatic solution in Sect. 3.5 at time $t = 0.15$ with 200×200 cells. 20 uniformly spaced contour lines from -0.0003 to 0.0003. *Left* results based on well-balanced method, *right* results based on non-well-balanced method

methods are not capable of capturing such small perturbation on the coarse mesh, while the well-balanced ones can resolve it very well. At the end, we also run the both methods on a refined mesh with 200×200 uniform cells, and show their pressure perturbation results in Fig. 7. The results of non-well-balanced DG methods are improving on the refined mesh, and the difference between well-balanced and non-well-balanced methods becomes smaller, which is what we expected.

3.6 Two-Dimensional Explosion Problem

In this last test case, we test a two-dimensional circular explosion problem following the setup in [4]. We consider an ideal gas ($\gamma = 1.4$) under the linear gravitational field with $\phi_x = 0, \phi_y = g = 0.118$, and the initial conditions

$$
\begin{aligned}
&\rho(x, y, t = 0) = 1, \\
&u(x, y, t = 0) = 0, \\
&v(x, y, t = 0) = 0, \\
&p(x, y, t = 0) = 1 - gy + \begin{cases} 0.005, & \text{if } (x - 1.5)^2 + (y - 1.5)^2 < 0.01, \\ 0, & \text{otherwise}, \end{cases}
\end{aligned}
$$

on the computational domain $[0, 3] \times [0, 3]$. Simple transmissive boundary conditions are used in all directions.

This test can also be viewed as a small perturbation of the steady state solution. We compute the solutions using both well-balanced and non-well-balanced DG methods, and compare their performance. Due to the circular pressure perturbation near the center of the domain, a shock wave will be developed, and propagate to the boundary. A uniform mesh of 100×100 computational cells is used, and we perform the simulation until $t = 2.4$. In Figs. 8 and 9, we plot the density ρ and velocity $\sqrt{u^2 + v^2}$ of both well-balanced and non-well-balanced methods at times $t = 1.2, 1.8$ and 2.4, where we can easily observe the big numerical error of non-well-balanced methods in the velocity plots. We would like to comment that although the underline steady state in this test does not have the form of (2.22), therefore our well-balanced methods are not designed to capture this steady state solution, but we can still observe the good behavior in capturing small perturbation of this equilibrium state.
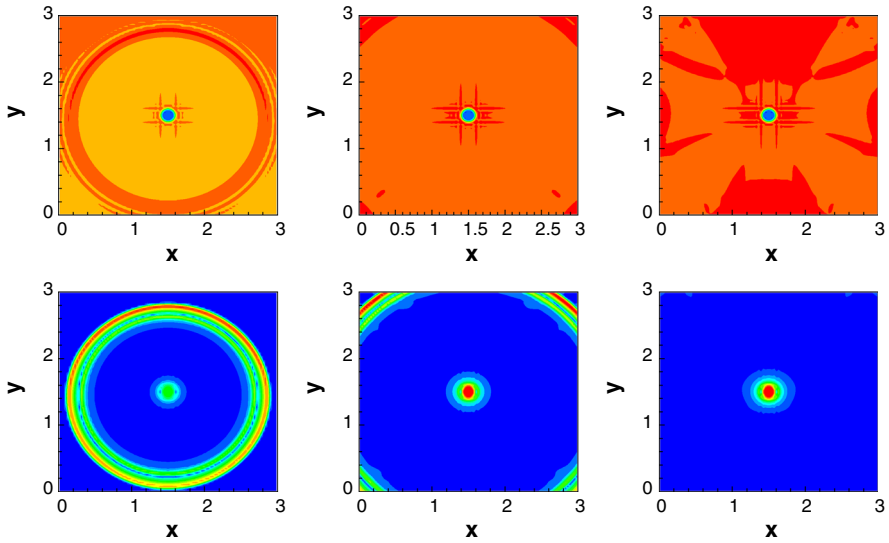
Fig. 8 The contours of the density and the velocity ($\sqrt{u^2 + v^2}$) of the explosion problem in Sect. 3.6 by well-balanced DG methods with 100×100 cells at times $t = 1.2$ (*left*), $t = 1.8$ (*middle*) and $t = 2.4$ (*right*). Ten uniformly spaced contour lines from 0.9955 to 1 for density and ten uniformly spaced contour lines from 0.2829 to 0.2838 for velocity. *Top* density, *bottom* velocity
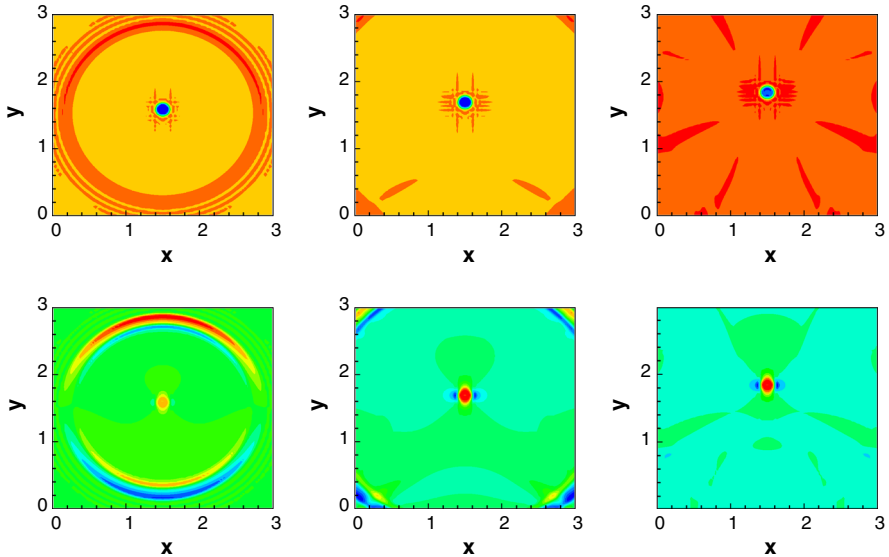
Fig. 9 The contours of the density and the velocity ($\sqrt{u^2 + v^2}$) of the explosion problem in Sect. 3.6 by non-well-balanced DG methods with 100×100 cells at times $t = 1.2$ (*left*), $t = 1.8$ (*middle*) and $t = 2.4$ (*right*). Ten uniformly spaced contour lines from 0.9955 to 1 for density and ten uniformly spaced contour lines from 0.2829 to 0.2838 for velocity. *Top* density, *bottom* velocity

4 Concluding Remarks

In this paper, we have constructed well-balanced DG methods for the isothermal equilibrium state solution of the Euler equations under static gravitational field. Special attention has been paid to the approximation of the source term, to achieve the well-balanced property. We have demonstrated that the proposed DG methods can balance the general isothermal equilibrium state exactly, and at the same time maintain the high order accuracy for the general solutions. Extensive numerical examples are provided to demonstrate the well-balanced property, accuracy, and good resolution of the proposed numerical methods for both continuous and discontinuous solutions. Another interesting equilibrium state of the Euler equations is the isentropic hydrostatic state. How to design high order well-balanced methods for such equilibrium and more general steady state constitutes our future work.

References

1. Audusse, E., Bouchut, F., Bristeau, M.-O., Klein, R., Perthame, B.: A fast and stable well-balanced scheme with hydrostatic reconstruction for shallow water flows. SIAM J. Sci. Comput. **25**, 2050–2065 (2004)
2. Bermudez, A., Vazquez, M.E.: Upwind methods for hyperbolic conservation laws with source terms. Comput. Fluids **23**, 1049–1071 (1994)
3. Botta, N., Klein, R., Langenberg, S., Lützenkirchen, S.: Well-balanced finite volume methods for nearly hydrostatic flows. J. Comput. Phys. **196**, 539–565 (2004)
4. Chertock, A., Cui, S., Kurganovz, A., Özcan, S.N., Tadmor, E.: Well-balanced central-upwind schemes for the Euler equations with gravitation. SIAM J. Sci. Comput., submitted
5. Cockburn, B., Karniadakis, G., Shu, C.-W.: The development of discontinuous Galerkin methods. In: Cockburn, B., Karniadakis, G., Shu C.-W. (eds.) Discontinuous Galerkin Methods: Theory, Computation and Applications. Lecture Notes in Computational Science and Engineering, Part I: Overview, vol. 11, pp. 3–50. Springer (2000)
6. Cockburn, B., Shu, C.-W.: The Runge–Kutta discontinuous Galerkin method for conservation laws V: multidimensional systems. J. Comput. Phys. **141**, 199–224 (1998)
7. Desveaux, V., Zenk, M., Berthon, C., Klingenberg, C.: A well-balanced scheme for the Euler equation with a gravitational potential. Finite Vol. Complex Appl. VII-Methods Theor. Asp. Springer Proc. Math. Stat. **77**, 217–226 (2014)
8. Greenberg, J.M., LeRoux, A.Y.: A well-balanced scheme for the numerical processing of source terms in hyperbolic equations. SIAM J. Numer. Anal. **33**, 1–16 (1996)
9. Kappeli, R., Mishra, S.: Well-balanced schemes for the Euler equations with gravitation. J. Comput. Phys. **259**, 199–219 (2014)
10. LeVeque, R.J.: Balancing source terms and flux gradients on high-resolution Godunov methods: the quasi-steady wave-propagation algorithm. J. Comput. Phys. **146**, 346–365 (1998)
11. LeVeque, R.J., Bale, D.S.: Wave propagation methods for conservation laws with source terms. In: Proceedings of the 7th International Conference on Hyperbolic Problems, pp. 609–618 (1998)
12. Luo, J., Xu, K., Liu, N.: A well-balanced symplecticity-preserving gas-kinetic scheme for hydrodynamic equations under gravitational field. SIAM J. Sci. Comput. **33**, 2356–2381 (2011)
13. Perthame, B., Simeoni, C.: A kinetic scheme for the Saint-Venant system with a source term. Calcolo **38**, 201–231 (2001)
14. Shu, C.-W.: TVB uniformly high-order schemes for conservation laws. Math. Comput. **49**, 105–121 (1987)

15. Shu, C.-W.: Total-variation-diminishing time discretizations. SIAM J. Sci. Stat. Comput. **9**, 1073–1084 (1988)
16. Slyz, A., Prendergast, K.H.: Time independent gravitational fields in the BGK scheme for hydrodynamics. Astron. Astrophy. Suppl. Ser. **139**, 199–217 (1999)
17. Tian, C.T., Xu, K., Chan, K.L., Deng, L.C.: A three-dimensional multidimensional gas-kinetic scheme for the Navier–Stokes equations under gravitational fields. J. Comput. Phys. **226**, 2003–2027 (2007)
18. Xing, Y.: Exactly well-balanced discontinuous Galerkin methods for the shallow water equations with moving water equilibrium. J. Comput. Phys. **257**, 536–553 (2014)
19. Xing, Y., Shu, C.-W.: High order finite difference WENO schemes with the exact conservation property for the shallow water equations. J. Comput. Phys. **208**, 206–227 (2005)
20. Xing, Y., Shu, C.-W.: High order well-balanced finite volume WENO schemes and discontinuous Galerkin methods for a class of hyperbolic systems with source terms. J. Comput. Phys. **214**, 567–598 (2006)
21. Xing, Y., Shu, C.-W.: A new approach of high order well-balanced finite volume WENO schemes and discontinuous Galerkin methods for a class of hyperbolic systems with source terms. Commun. Comput. Phys. **1**, 100–134 (2006)
22. Xing, Y., Shu, C.-W.: High order well-balanced WENO scheme for the gas dynamics equations under gravitational fields. J. Sci. Comput. **54**, 645–662 (2013)
23. Xing, Y., Shu, C.-W.: A survey of high order schemes for the shallow water equations. J. Math. Study **47**, 221–249 (2014)
24. Xing, Y., Zhang, X., Shu, C.-W.: Positivity-preserving high order well-balanced discontinuous Galerkin methods for the shallow water equations. Adv. Water Resour. **33**, 1476–1493 (2010)
25. Xu, K.: A well-balanced gas-kinetic scheme for the shallow-water equations with source terms. J. Comput. Phys. **178**, 533–562 (2002)
26. Xu, K., Luo, J., Chen, S.: A well-balanced kinetic scheme for gas dynamic equations under gravitational field. Adv. Appl. Math. Mech. **2**, 200–210 (2010)
27. Zingale, M., Dursi, L.J., ZuHone, J., Calder, A.C., Fryxell, B., Plewa, T., Truran, J.W., Caceres, A., Olson, K., Ricker, P.M., Riley, K., Rosner, R., Siegel, A., Timmes, F.X., Vladimirova, N.: Mapping initial hydrostatic models in Godunov codes. Astrophys. J. Suppl. Ser. **143**, 539–565 (2002)